Chapter 4: Transparent and Flexible Quantum Dot-Polymer Composites Using an Ionic Liquid as Compatible Polymerization Medium

Chapter Summary

Quantum dots (QDs)-polymer composites were fabricated based on a solution of QDs dispersed in an ionic liquid. Positively charged water-soluble nanocrystals were obtained from solutions of CdSe/ZnS QDs dispersed in toluene by ligand exchange with 2-dimethylaminoethanethiol (DAET). The resulting QDs were further transferred into a hydrophobic ionic liquid HMITFSI (1-Hexyl-3-methylimidazolium bis(trifluoromethylsulfonyl)imide) by cation exchange, resulting in a CdSe/ZnS-HMITFSI solution, which was used as a compatible medium for the polymerization and cross-linking of poly(methylmethacrylate) networks. Transparent and fluorescent materials resulted. The quantum yields of the composites depended on the initial properties of the QDs dispersed in toluene, and medium size QDs (2.6 nm) resulted in the highest quantum yields.

4.1 Introduction

Semiconductor nanocrystals presenting size-dependent optical properties arising from their quantum confinement have attracted great interest in recent years. In particular, incorporating quantum dots (QDs) into polymeric matrices has been the subject of intense research efforts. These organic-inorganic composites are promising materials for new generations of optical[1], nonlinear optical[2,3], electronic devices[4,5] and biological labels[6,7]. One of the challenges involved in the synthesis of these materials is the inherent incompatibility of the quantum dots with the polymer matrix, which is responsible for aggregation of the nanoparticles, loss of transparency of the composite, and quenching of the embedded quantum dot fluorescence. Several methods have already being described to overcome this problem. A number of studies described the direct synthesis of quantum dots inside a polymer matrix and the nonlinear optical

properties of the resulting films. Du et al.[8] synthesized CdS nanocrystals inside a sulfonated polystyrene matrix. The SO_3^- ions formed within the matrix provided sites for the growth of CdSe quantum dots, which were obtained by aggregation of cadmium ions and subsequent reaction with S^{2-} ions supplied by thioacetamide. They observed that the nonlinear refractive index of the composite decreased as the input irradiance increased. Similarly, significant work was performed on the synthesis of quantum dots inside Nafion films by ion-exchange. He et al.[3] measured the two-photon absorption coefficient and the optical Kerr coefficient in CdS-Nafion composites synthesized by soaking Nafion membranes in an aqueous solution of cadmium acetate followed by hydrogen sulfide gas treatment. They noticed that the quantum dots were mostly located near the surfaces of the resulting hybrid films. Similarly, Wang et al. demonstrated large third-order nonlinearities in CdS-Nafion films.

Quantum dot-polymer composites may also be produced by polymerizing polymer monomers mixed with pre-synthesized quantum dots. Lee et al.[9] demonstrated the fabrication of quantum dot-poly(laurylmethacrylate) composites by mixing TOP (TriOctylPhosphine) covered CdSe/ZnS with a laurylmethacrylate monomer, followed by polymerization of the resulting solution. They were able to build a light-emitting device based on their resulting material. Another approach consisted of using ligands possessing a moiety similar to the matrix monomer. For example, Erskine et al.[10] demonstrated the copolymerization of 4-thiomethylstyrene covered CdSe quantum dots with a styrene monomer.

Skaff et al. performed a number of studies on the synthesis of tailored ligands composed of a moiety capable of interacting with the quantum dot surface and at the same time suitable for copolymerization or covalent attachment of a polymeric component. They applied this technique to the fabrication of CdSe covered with PEG substituted pyridine ligands[11], CdSe-polyolefin composites[12] and CdSe-Poly(*para*-phenylene vinylene) composites[13]. Likewise, Zhang et al.[14,15] used two related techniques to fabricate CdTe-polymer composites. Their first method involved the extraction of negatively charged water-soluble CdTe quantum dots into a styrene monomer using the surfactant octadecyl-*p*-vinyl-benzyldimethylammonium chloride (OVDAC), followed by the copolymerization of the surfactant and the monomer. Their second method consisted of

copolymerizing the OVDAC and the styrene monomer first and coating the quantum dots afterwards.

Most of the approaches described above involve complex synthesis of polymerizable surfactants or ligands, or pre-processing steps like sulfonation of the polymer matrix. Moreover, no study has been reported so far which depicts a convenient synthetic route for producing flexible polymer-quantum dot-bulk composites or self-standing films, which may lead to the manufacture of flexible electronic components, optical and nonlinear optical devices, etc.

In this chapter, we describe an alternative method for incorporating quantum dots into a polymer matrix, which utilizes the extraction of positively charged water soluble nanocrystals into a hydrophobic ionic liquid by cation transfer[16,17]. The ionic liquid/quantum dot solution is used as a compatible medium for the polymerization and cross-linking of poly(methylmethacrylate) (PMMA) to provide a transparent polymer network-ionic liquid/quantum dot composite whose flexibility may be tailored by varying the ionic liquid content. This technique provides a straightforward approach to fabricate rigid or flexible transparent bulk composites or self-standing films, while avoiding complicated processing steps previously described. The inherent incompatibility of quantum dots with polymers is overcome, as the nanocrystals are dispersed in the ionic liquid, which is totally compatible with the polymer network[18,19]. Our approach may be applicable to any compatible radical polymer/hydrophobic ionic liquid system, where the ionic liquid is suitable for the extraction of positively charged quantum dots, thereby making this method very general.

4.2 Experimental Section

4.2.1 Materials.

CdSe/ZnS quantum dots (QDs) dispersed in toluene with emission wavelengths of 520 nm (light green emitting, 2.1 nm), 558 nm (green emitting, 2.6 nm) and 598 nm (orange emitting, 4 nm) were obtained from Evident Technologies and NN-Labs. 2-dimethylaminoethanethiol (DAET), methyl methacrylate (MMA), 2,2'-

azobisisobutyronitrile (AIBN) as initiator and ethylene glycol dimethacrylate (EGDMA) as cross-linker were purchased from Sigma-Aldrich. 1-hexyl-3-methyl imidazolium bis(trifluoromethane sulfonyl)imide (HMITFSI) (Figure 4.1) was purchased from EMD Chemicals. The deionized water used was from an 18-MΩ Barnstead Nanopure water system. All the chemicals were used without further purification.

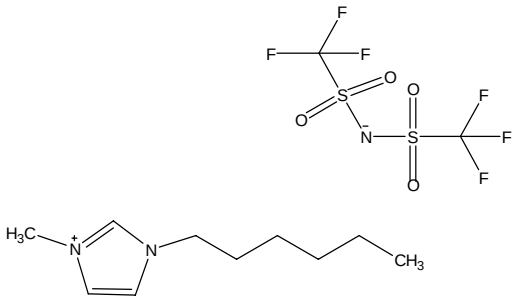

Figure 4.1. 1-Hexyl-3-methylimidazolium bis(trifluoromethylsulfonyl)imide.

4.2.2 Preparation of Water-Soluble CdSe/ZnS Quantum Dots.

Water-soluble CdSe/ZnS QDs were obtained by adding methanolic solutions of 2-dimethylaminoethanethiol (DAET) to 1mL of the initial solutions of QDs dispersed in toluene, until the nanocrystals flocculated. 2M, 1M and 0.5M DAET methanolic solutions were respectively added to the light green, green, and orange emitting QDs toluene solutions. As soon as the particles flocculated, 1mL of deionized water was added to the solutions, resulting in a two-phase system with the water phase below the toluene phase. After stirring and decanting, the QDs were extracted into the water phase.

4.2.3 Extraction of the CdSe/ZnS QDs into HMITFSI.

The water-soluble CdSe/ZnS QDs were further extracted into HMITFSI by mixing each hydrophilic QDs solution to an equivalent volume of the hydrophobic ionic liquid. After stirring and decanting, CdSe/ZnS were transferred into the ionic liquid by cation exchange[16,17]. The resulting solutions were heated in a vacuum oven at 70ºC for 30 min to eliminate any remaining traces of water and methanol, which led to the formation of transparent solutions.

4.2.4 Synthesis of the PMMA-HMITFSI/CdSe/ZnS Composites.

The HMITFSI/QD solutions were mixed with methylmethacrylate with a 4:7 molar ratio of HMITFSI/QD to monomer for the rigid composites and a 6:5 molar ratio of HMITFSI/QDs to monomer for the flexible ones. 0.4 mol% AIBN and 2 mol% EGDMA were further added, and the resulting solutions transferred into 5mL glass vials and 30mm×2mm squared glass tubes and polymerized in an air oven for 20 min at 90ºC, followed by 8h at 65ºC. Transparent composites resulted.

4.2.5 Characterization.

Fluorescence measurements of all solutions and composites were performed with a Hitachi-F-4500 spectrofluorimeter. UV-vis absorption spectra were recorded with a Shimadzu UV-2501 PC spectrophotometer. Thermogravimetric analysis of the samples was carried out on a Q500 Texas Instrument thermogravimetric analyzer. The samples were heated from room temperature to 700ºC at a heating rate of 10ºC/min in open platinum pans, under a nitrogen atmosphere. Differential Scanning Calorimetry (DSC) experiments were performed on a Q1000 Texas Instrument Differential Scanning Calorimeter. The samples were heated in closed aluminum pans under a nitrogen atmosphere to 200ºC, cooled to -150ºC and heated again to 200ºC at a cooling and heating rate of 10ºC/min. The relative quantum yields of the different solutions and composites were estimated by comparison with the standard fluorescent dye Rhodamine 6G.[9,15] The difference in refractive index of the different solutions was taken into account, and care was taken to ensure reproducible instrumental conditions. The quantum yields were determined from the following formula for the solutions and composites involving the green emitting QDs:

$$QY\% = \left(\frac{\Delta\Psi_s}{\Delta\Psi_{Rh}}\right)\left(\frac{\eta_s}{\eta_{Rh}}\right)^2 qy_{Rh} \qquad (4.1)$$

where $\Delta\Psi_s$ and $\Delta\Psi_{Rh}$ are derived from the fluorescence spectra by integrating the emitted intensity over the chosen spectral range for the sample and rhodamine 6G respectively, for equal absorbances. The terms η_s and η_{Rh} represent the refractive indexes of the

dispersion medium of the QDs and rhodamine 6G; qy_{Rh} represents the quantum yield of the standard, which is 95% for rhodamine 6G. For the solutions and composites involving the light green and orange emitting QDs, the quantum yields were obtained relatively to the quantum yields of the samples involving green emitting QDs, from the following formula:

$$QY_{\lambda}\% = \left(\frac{\Delta\Psi_{\lambda}}{\Delta\Psi_{green}} \right) QY_{green} \qquad (4.2)$$

where $\Delta\Psi_{\lambda}$ and $\Delta\Psi_{green}$ are the integrated fluorescence emission intensities for the light green or orange emitting QDs and the green emitting QDs respectively, for equal absorbances.

4.3 Results and Discussion

4.3.1 Fabrication of PMMA/HMITFSI/CdSe/ZnS Composites

A general preparation method is depicted in Figure 4.2. The transfer of the quantum dots into the hydrophobic ionic liquid requires the QDs to be positively charged and dispersed into water. This was achieved by exchanging the ligand of the quantum dots initially dispersed in toluene for a positively charged and water-soluble ligand. 2-dimethylaminoethanethiol was chosen as a suitable capping ligand because of its high melting point comprised between 150 and 160ºC, to avoid alteration of the ligand during the polymerization of the composites. The higher affinity of the thiol groups of 2-dimethylaminoethanethiol for the surface of the QDs compared to the initial ligand of the QDs dispersed in toluene readily led to a capping exchange on the surface of the QDs. Once the ligand exchange had taken place, the QDs became hydrophilic and no longer soluble in toluene, which led to their flocculation inside the solvent and enabled their subsequent extraction into water. The positively charged water soluble QDs could then easily be transferred from water to HMITFSI via cation exchange[16,17] as shown in Scheme 4.1. Once the QDs were dispersed in the ionic liquid, the resulting solution was

used as a compatible medium for the fabrication of PMMA networks, which led to transparent and fluorescent composites.

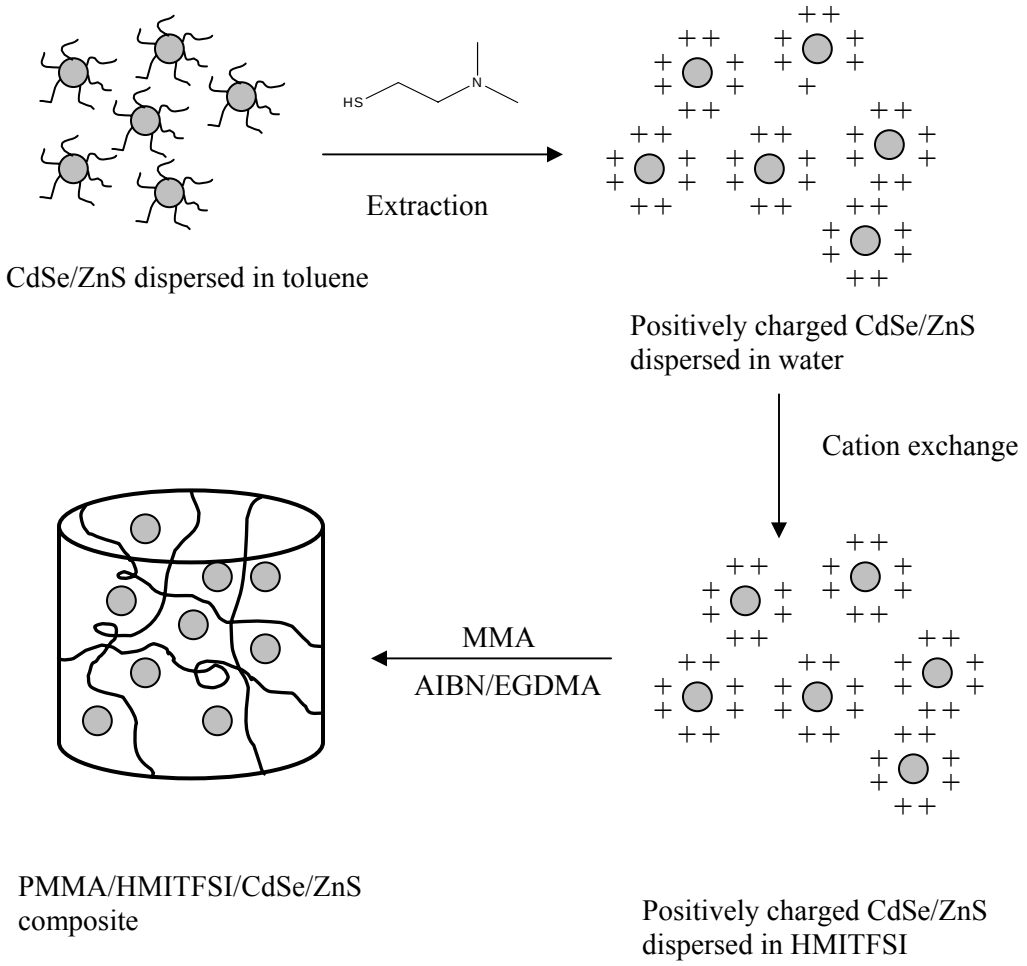

Figure 4.2. Fabrication method of the transparent and fluorescent PMMA/HMITFSI/CdSe/ZnS composites.

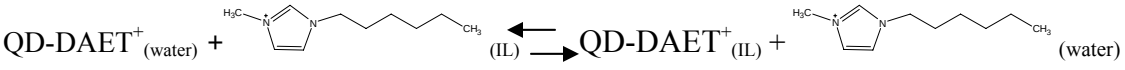

Scheme 4.1. Cation exchange process.

Figure 4.3, 4.4 and 4.5 represent the normalized fluorescence and absorbance spectra of the different color emitting QDs dispersed in toluene, in water after ligand

exchange with DAET, and in the ionic liquid for an excitation wavelength of 450 nm. It was observed that the shape of the emission spectra of the QDs transferred into water was similar to the shape of the emission spectra of the QDs dispersed in toluene, as previously described for the transfer of QDs from chloroform to water by capping exchange[20]. Both emission spectra exhibited narrow full width at half maximum (FWHM) (Table 4.2), and quantum size effect for all three color emitting QDs. The size distribution of the nanocrystals dispersed in water thus remained nearly similar to the size distribution of the QDs dispersed in toluene.

Small blue shifts of the absorbance spectra of the three colors emitting QDs were noticed. This was similar to the results of Wuister et al.[20] who observed a significant blue shift for water-soluble CdTe QDs capped with aminoethanethiol. They explained this shift by a redistribution of the electronic density and increase in the confinement energy of the QDs attributed to the stronger Cd-thiol bond when compared to the Cd-amine bond. The reduced blue shift in our results may be attributed to the protecting ZnS shell present on the surface of the CdSe/ZnS QDs, which may diminish the difference in strength between the two types of bonds.

Although thiol capping was previously observed to quench the fluorescence of CdSe quantum dots[21], the ZnS shell present on the surface of the CdSe/ZnS QDs protected the CdSe core from trapping of the photogenerated hole on the thiol groups, which has been shown to hinder the radiative recombination of the exciton[21]. Likewise, Hines et al.[22] observed that CdSe/ZnS QDs did not undergo fluorescence quenching when the TOPO ligands of the QDs were replaced by pyridine, which usually quenches the fluorescence of CdSe QDs. The fluorescence of the CdSe/ZnS QDs was thus well preserved, and high quantum yields were obtained for the light green and green-emitting QDs dispersed in water (see Table 4.1). The difference in quantum yields between the three different color emitting QDs, and the significantly lower quantum yield of the orange emitting QDs may be explained by a disparity in the quality of the QDs surfaces. The growth of QDs usually occurs through Ostwald ripening where larger particles are built through the consumption of monomer released by the dissolution of smaller particles[23-25]. The largest or smallest nanocrystals present more surface defects acting as traps for photogenerated carriers[26] than medium size ones, which may be explained by a

difference in the growth kinetics of the different fractions of nanocrystals. The nanoparticles having an average growth rate close to zero present the lowest number of surface defects, while nanoparticles with a positive growth rate (larger sizes) or nanoparticles with a negative growth rate (smaller sizes) possess surfaces with numerous defects[24,25]. The same authors found that the best core-shell nanocrystals were prepared from the best core nanocrystals, thus it may be assumed that the CdSe/ZnS QDs used in this study present surface qualities determined from their growth rate, similarly to their corresponding core QDs. The defects present on the surface of QDs are mostly dangling bonds and crystal defects, which are hindering the direct recombination of the electrons into the valence band after they have been excited across the bandgap and into the conduction band by a photon flux. The decaying of some of the recombination electrons will induce a reduction in the photon flux emitted. The lower quantum yield of the orange emitting QDs dispersed in water was coupled with a narrowing of the fwhm of their emission spectrum. The FWHM was 37 nm for QDs dispersed in toluene, while it was 30 nm for QDs dispersed in water.

No noticeable change could be detected in the shape of the emission and absorbance spectra of the light green and green emitting QDs once they were transferred in HMITFSI suggesting that the cation exchange process from water to HMITFSI did not affect their surface quality or their size dispersion. The FWHM remained the same for the three different color emitting QDs. A blue shift was observed in the emission spectra of the orange emitting QDs dispersed in HMITFSI when compared to their emission spectra in water (Table 4.2). This difference was ascribed to the better stability of the thiol groups in the ionic liquid than in water, rendering the Cd-thiol chemical bond stronger in the ionic liquid, which leads to an increase in the confinement energy of the QDs as previously mentioned. The increased stability of the thiol groups in the ionic liquid may be explained by the absence of hydration of the thiolate anions, which has been shown to be responsible for their dissociation from the QDs in an aqueous environment.[16,27] It was observed that aqueous solutions of light green and green emitting QDs were stable when compared to aqueous solutions of orange emitting QDs, which confirmed the difference in stability of the thiol bonds for the different solutions of QDs, and was responsible for the absence of blue shift for the light green and green emitting

QDs, when transferred in HMITFSI (Table 4.2). It may be postulated that the higher amount of surface defects present on the surface of the larger size QDs lowered the strength of the Cd-thiol bond.

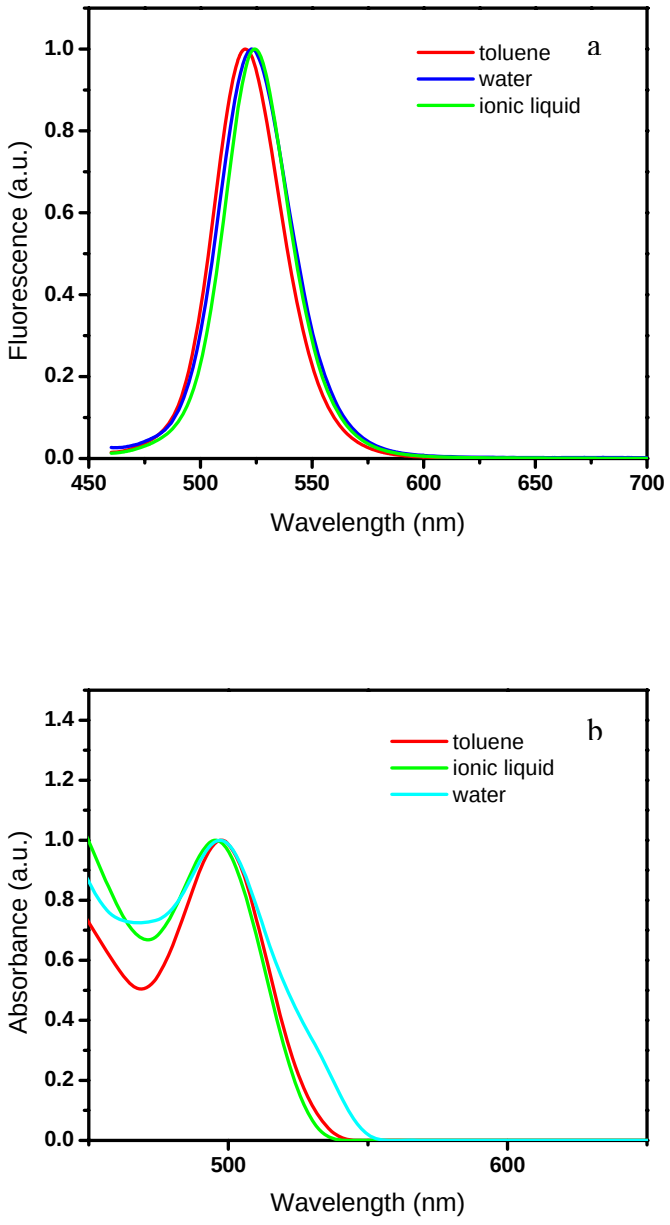

Figure 4.3. a) Emission spectra of the light green emitting QDs dispersed in toluene, water and ionic liquid, λ_{ex}=450 nm. b) Absorbance spectra of the light green emitting QDs dispersed in toluene, water and ionic liquid.

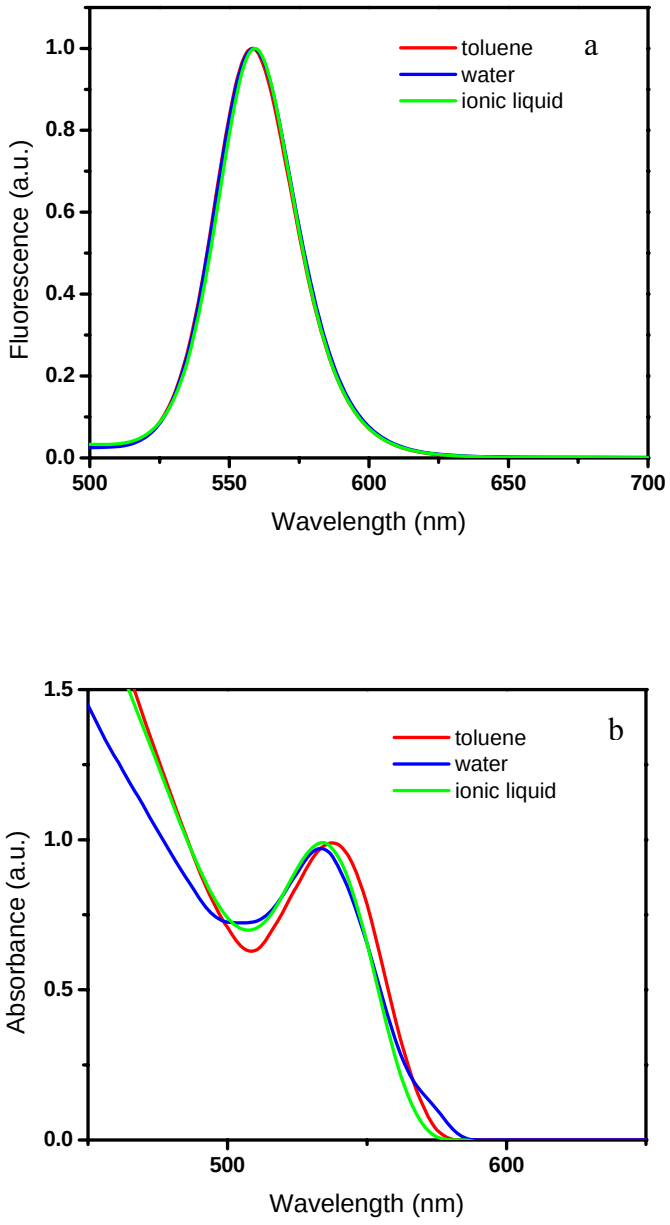

Figure 4.4. a) Emission spectra of the green emitting QDs dispersed in toluene, water and ionic liquid. b) Absorbance spectra of the green emitting QDs dispersed in toluene, water and ionic liquid.

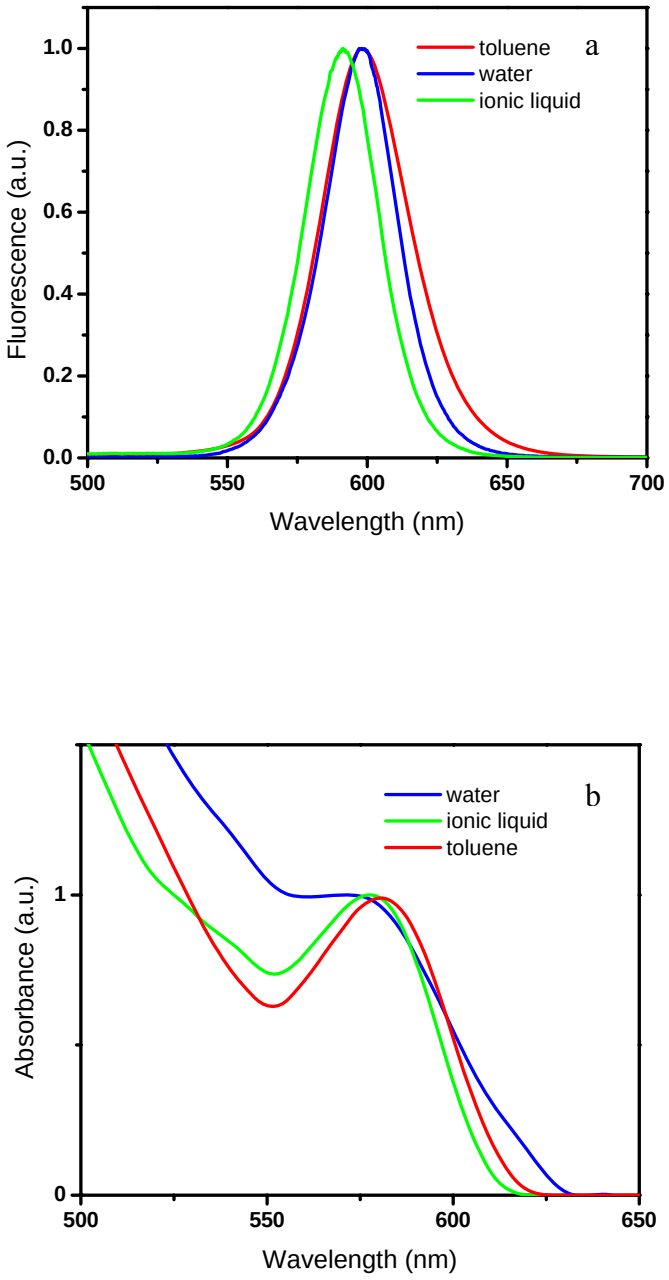

Figure 4.5. a) Emission spectra of the orange emitting QDs dispersed in toluene, water and ionic liquid. b) Absorbance spectra of the orange emitting QDs dispersed in toluene, water and ionic liquid.

The improved stability of the thiol groups in the ionic liquid also accounted for the increased quantum yields of the QDs dispersed in HMITFSI when compared to the QDs dispersed in water (Table 4.1). A 46% and 65% increase in quantum yield was observed for the green and light green QDs respectively. The quantum yield of the orange emitting QDs dispersed in HMITFSI was more than two times higher than the quantum yield of the orange emitting QDs dispersed in water. This may be explained by an increased instability of the thiol groups attached to the surface of the orange emitting QDs dispersed in water after ligand exchange, attributed to the decreased surface quality of the larger size QDs as previously described. The instability of the thiol group induces some aggregation of the QDs, which in turn leads to an increased absorbance. As the quantum yield is determined from the ratio of the amount of photons emitted by a sample to the ratio of the amount of photons absorbed by a sample, an increased amount of photon absorbed will lead to a reduced ratio, and a reduced quantum yield. The solutions of QDs dispersed in HMITFSI were produced by cation-exchange with freshly produced solutions of QDs dispersed in water, which may explain the high value for the quantum yield of the orange emitting QDs dispersed in HMITFSI despite the significantly lower value of the quantum yield for the orange emitting QDs dispersed in water. Likewise, Kurth et al.[28] demonstrated that covering CdTe QDs with the surfactant dimethyldioctadecylammonium bromide almost doubled their emission intensity, which they attributed to a similar increase in the stability of the surfaces of the QDs covered by the surfactant. No precipitation of the different solutions of QDs dispersed in HMITFSI was observed and the solutions were stable and transparent for several months, which confirmed the stabilizing and protective role of the ionic liquid. Figure 4.6 shows a picture of the QDs dispersed in HMITFSI and exposed under an UV light. Another factor, which may further enhance the quantum yield of the QDs dispersed in HMITFSI is the heat treatment that was applied on the QDs after their transfer from water to HMITFSI, as described in the experimental section. Heat has been proved to enhance the quantum yield of QDs by correcting the defects present at the surface of the nanocrystals[16].

Figure 4.6. a) Transparent solutions of CdSe/ZnS QDs dispersed in HMITFSI. b) Fluorescence images of the three color emitting CdSe/ZnS QDs dispersed in HMITFSI and exposed under an ultraviolet lamp.

Table 4.1. Emission peaks of the CdSe/ZnS QDs dispersed in toluene, water, ionic liquid and composites.

Emitting color and size (nm)	In toluene (nm)	In water (nm)	In HMITFSI (nm)	In composite (nm)
Light green (2.1)	520	523	524	521
Green (2.6)	558	559	559	559
Orange (4)	598	597	591	592

Table 4.2. Quantum yields of the CdSe/ZnS QDs dispersed in toluene, water, ionic liquid and composites.

Emitting color and size (nm)	In toluene (%)	In water (%)	In HMITFSI (%)	In composite (%)
Light green (2.1)	50	38	63	22
Green (2.6)	50	41	60	38
Orange (4)	18	8	19	9

Figure 4.7 represents the fluorescence and absorbance spectra of the composites obtained for the three color emitting QDs. The emission peaks of the CdSe/ZnS QDs in the composites remained similar to the emission peaks of the QDs dispersed in HMITFSI (Table 4.2), suggesting that the properties of the QDs dispersed in the composites were similar to the properties of the QDs dispersed in HMITFSI. No aggregation or precipitation of the QDs took place during the polymerization of the composites as shown in Figure 4.8, and as demonstrated by the fluorescence spectra in Figure 4.7.

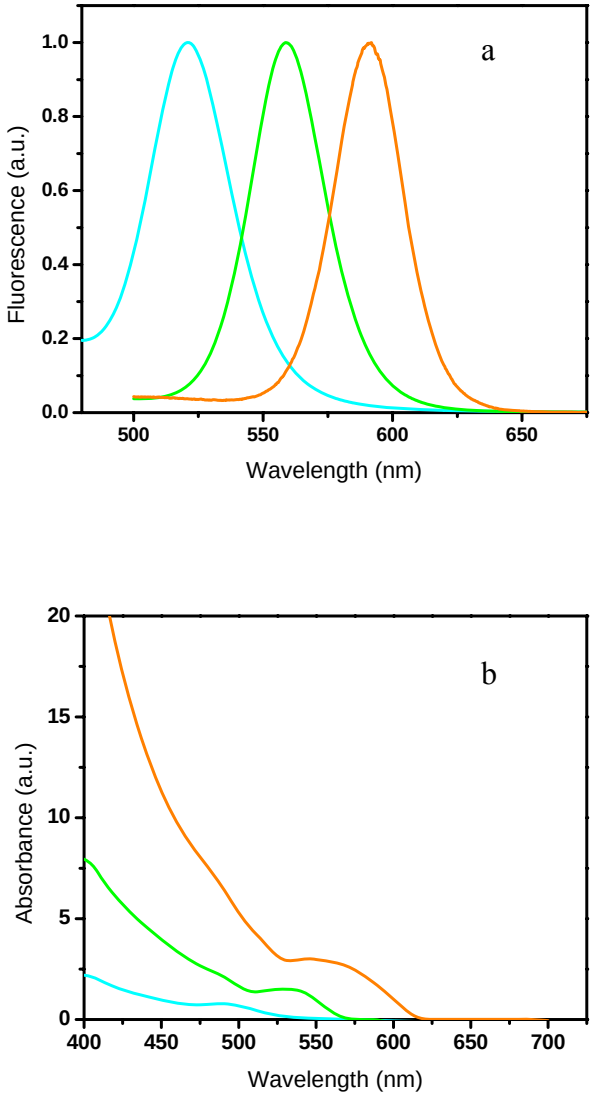

Figure 4.7. a) Fluorescence of the CdSe/ZnS/HMITFSI/PMMA composites. b) Absorbance spectra of the CdSe/ZnS/HMITFSI/PMMA composites.

The quantum yields of the resulting composites depended on the initial quantum yields of the QDs dispersed in toluene, and on the surface quality of the initial QDs. The highest quantum yields were obtained for the composites fabricated with green emitting QDs, which were the QDs presenting the highest surface quality due to their medium size corresponding to a zero average growth rate[24], while the lowest quantum yield was obtained for the orange emitting QDs presenting the lowest surface quality associated with their larger size corresponding to a positive growth rate. The orange emitting QDs presented the lowest initial quantum yield when dispersed in toluene, which was another factor resulting in the low quantum yield of the composites. Although the quantum yields of the light green and green emitting QDs dispersed in the composites were lower than the quantum yields of the QDs dispersed in the ionic liquid, they remained significantly high. The decrease in quantum yield was attributed to the free-radicals produced from AIBN during the polymerization phase.[14]

Figure 4.8. a) Transparent CdSe/ZnS-HMITFSI-PMMA composites fabricated with a 4:7 molar ratio of HMITFSI/QDs to MMA. b) Differently shaped composites exposed under an ultraviolet lamp. c) Curved composites fabricated with a 6:5 molar ratio of HMITFSI/QDs to MMA.

The concentration of QDs present in each composite was determined by TGA. Concentrations of 1.29, 2.60 and, 1.26 wt.% were obtained for the composites based on light green, green and orange emitting QDs respectively. The composites were insoluble in organic solvents like chloroform or dichloromethane, indicating successful cross-linking of the polymer by EGDMA.

Figure 4.9 shows a representative TGA curve for a HMITFSI/QDs-PMMA composite along with the TGA curves of pure HMITFSI and pure PMMA. The thermal stability of the composite was comprised between the thermal stability of pure PMMA and the high thermal stability of pure HMITFSI. Two weight-loss steps were noticed for the HMITFSI/QDs-PMMA composite, the first one corresponding to the decomposition of cross-linked PMMA, and the second one corresponding to the decomposition of HMITFSI present in the network, similarly to results obtained for other ionic liquid-polymer systems.[18,19] The first weight loss step of the composite started at 267ºC, while the second one started at 307ºC. The ionic liquid started to decompose at 315ºC, while pure PMMA started to decompose at 200ºC. Two weight-loss steps were noticed for pure PMMA. The first weight loss corresponded to unreacted MMA monomer, while the second one starting at 255ºC was attributed to PMMA.

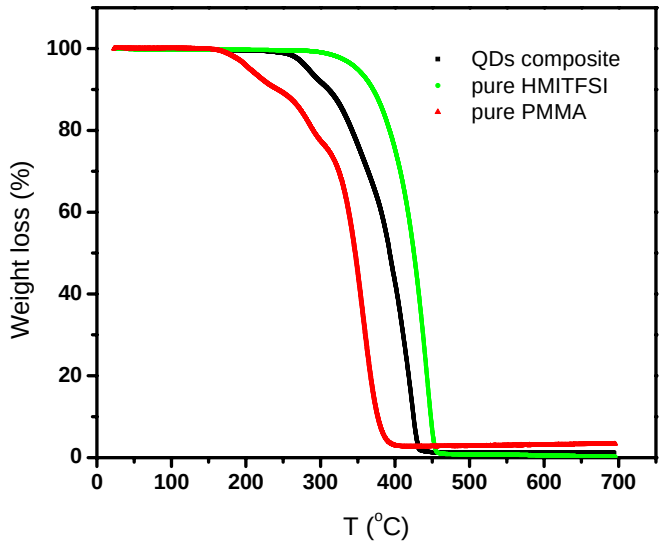

Figure 4.9. TGA curves for the HMITFSI/QDs-PMMA composites, pure HMITFSI, and pure PMMA.

Figure 4.10 represents a typical DSC curve for an HMITFSI-PMMA composite, along with the DSC curves of pure HMITFSI and pure PMMA. The DSC experiments were performed on composites, which did not include CdSe/ZnS QDs, to avoid interference with the QDs ligand (DAET). It was observed that the sharp endothermic peak present in the DSC curve of the pure ionic liquid (T_m=-8º) did not appear in the DSC curve of the composite, as previously observed for another polymer-ionic liquid system[19]. The glass transition temperature peak (Tg=-88ºC) present for the pure ionic liquid and the glass transition temperature peak for PMMA were difficult to notice in the composite, which was also in agreement with previously obtained results.

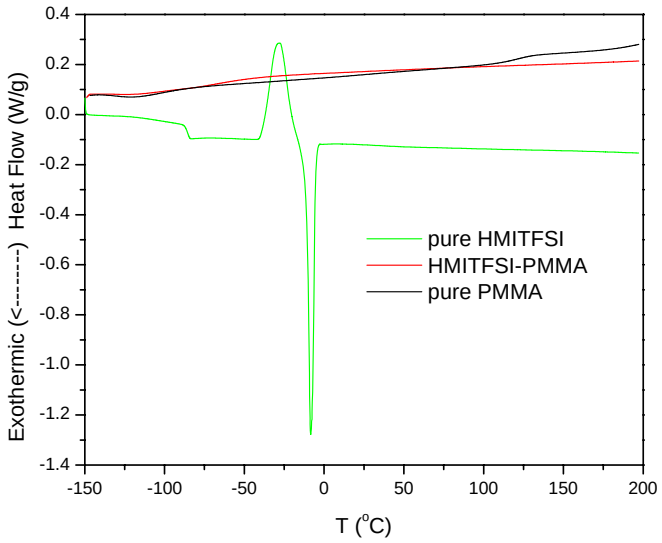

Figure 4.10. DSC curves for the HMITFSI-PMMA composites, pure HMITFSI, and pure PMMA.

4.4 Conclusions

In summary, we have described a convenient method for fabricating rigid or flexible polymer-quantum dot composites. These hybrid materials were synthesized by extracting positively charged CdSe/ZnS quantum dots into a hydrophobic ionic liquid, which was used as a compatible medium for the polymerization and cross-linking of PMMA networks. We obtained transparent and fluorescent composites, which may be

used in new types of electronic or optical devices and applications. The composites fabricated presented quantum yields, which depended on the initial properties of the QDs. The highest quantum yields were obtained for composites fabricated with medium size (green emitting) quantum dots. Our method may be extended to any compatible radical polymer-ionic liquid system, as well as potentially to other compatible polymer-ionic liquid systems, where the cross-linking of the polymer may be initiated by external physical means such as UV exposure.

4.5 References

(1) Colvin, V. L., Schlamp, M. C., Alivisatos, A. P. *Nature* **1994**, *370*, 354-357.

(2) Klimov, V. I., Mikhailovsky, A. A., Xu, S., malko, A., Hollingsworth, J. A., Leatherdale, C. A., Eisler, H. J., Bawendi, M. G. *Science* **2000**, *290*, 314-317.

(3) He, J., Ji, W., Ma, G. H., Tang, S. H. , Kong, E. S. W. , Chow, S. Y. , Zhang, X. H. , Hua, Z. L. , and Shi, J. L. *Journal of Physical Chemistry B* **2005**, *109*, 4373-4376.

(4) Gao, M., Lesser, C., Kirstein, S., Mohwald, H., Rogach, A. L., Weller, H. *Journal of Applied Physics* **2000**, *87*, 2297-2302.

(5) Tessler, N., Medvedv, V., Kazes, M., Kan, S. H., Banin, U. *Science* **2002**, *295*, 1506-1508.

(6) Bruchez, M. P., Moronne, M., Weiss,S., Alivisatos, A. P. *Science* **1998**, *281*, 2013-2016.

(7) Poznyak, S. K., Talapin, D. V., Shevchenko, E. V., Weller H. *Nano Letters* **2004**, *4*, 693-698.

(8) Du, H., Xu, G. Q., Chin, W. S., Huang, L., and Ji, W. *Chemistry of Materials* **2002**, *14*, 4473-4479.

(9) Lee, J., Sundar V. C., Heine, J. R.,Bawendi, M. G., and Jensen, K. F. *Advanced Materials* **2000**, *12*, 1102-1105.

(10) Erskine, L., Emrick, T., Alivisatos, A. P., and Frechet, J. M. *Polymer Preprint* **2000**, *41*, 593.

(11) Skaff, H., and Emrick, T. *Chemical Communications* **2003**, 52-53.

(12) Skaff, H., Firat Ilker, M., Bryan Coughlin, E., and Emrick, T. *Journal of the American Chemical Society* **2002**, *124*, 5729-5733.

(13) Skaff, H., Sill, K., and Emrick, T. *Journal of the American Chemical Society* **2004**, *126*, 11322-11325.

(14) Zhang, H., Wang, C., Li, M., Ji, X., Zhang, J., and Yang, B. *Chemistry of Materials* **2005**, *17*, 4783-4788.

(15) Zhang, H., Cui, Z., Wang, Y., Zhang, K., Ji, X., Lu, C., Yang, B., and Gao, M. *Advanced Materials* **2003**, *15*, 777-780.

(16) Nakashima, T., and Kawai, T. *Chemical Communications* **2005**, 1643-1645.

(17) Dietz, M. L., and Dzielawa, J. A. *Chemical Communications* **2001**, 2124-2125.

(18) Snedden, P., Cooper, A. I., Scott, K., and Winterton, N. *Macromolecules* **2003**, *36*, 4549-4556.

(19) Susan, M. A. B. H., Kaneko, T., Noda, A., and Watanabe, M. *Journal of the American Chemical Society* **2005**, *127*, 4976-4983.

(20) Wuister, S. F., Swart, I., van Driel, F., Hickey, S. G., and Donega, C. de M. *Nano Letters* **2003**, *3*, 503-507.

(21) Wuister, S. F., Donega, C. de M., and Meijerink, A. *Journal of Physical Chemistry B* **2004**, *108*, 17393-17397.

(22) Hines, M. A., and Guyot-Sionnest, P. *Journal of Physical Chemistry* **1996**, *100*, 468-471.

(23) Ostwald, W. Z. *Physical Chemistry* **1901**, *37*, 385.

(24) Talapin, D. V., Rogach, A. L., Shevchenko, E. V., Kornowski, A., Haase, M., and Weller, H. *Journal of the American Chemical Society* **2002**, *124*, 5782-5790.

(25) Talapin, D. V., Rogach, A. L., Haase, M., Weller, H. *Journal of Physical Chemistry B* **2001**, *105*, 12278-12285.

(26) Resch, U., Weller, H., Heinlein, A. *Langmuir* **1989**, *5*, 1015-1020.

(27) Hohng, S., and Ha, T. *Journal of the American Chemical Society* **2004**, *126*, 1324-1325.

(28) Kurth, D. G., Lehmann, P., and Lesser, C. *Chemical Communications* **2000**, *11*, 949-950.